Acta virologica **64**: 44 – 58, 2020 doi: 10.4149/av_2020_106

Thiol/disulfide exchange occurs in rotavirus structural proteins during contact with intestinal villus cell surface

M. RIVERA, C. A. GUERRERO*, O. ACOSTA

Departamento de Ciencias Fisiológicas, Facultad de Medicina, Universidad Nacional de Colombia, Bogotá, DC., Colombia

Received January 10, 2019; revised August 28, 2019; accepted January 11, 2020

Summary. – Protein disulfide isomerase (PDI) is an enzyme that catalyzes disulfide bond reduction or formation and rearrangements of disulfide bridges, and also functions as a chaperone. During entry of some of the viruses PDI participates in thiol-disulfide exchange. Previous reports show that rotavirus entry is interfered by impermeant thiol/disulfide exchange inhibitors and antibodies against PDI. Our objective was to assess the interaction between PDI and triple-layered particles (TLPs) from rotavirus strains ECwt and RRV and from a human rotavirus isolate (HI) during the early steps of virus entry in a system of isolated small intestinal villi. Purified soluble PDI was incubated with either isolated intestinal villi or cell membrane-enriched fractions in the presence or absence of thiol/disulfide inhibitors such as bacitracin, DTNB or N- ethylmaleimide followed by the assessment of the PDI interactions with TLPs and rotavirus structural proteins in terms of their redox state changes. Soluble and membrane-bound PDI was found to interact with TLPs from all the rotaviruses assayed and also with the isolated structural proteins represented by the recombinant rVP5* (a tryptic cleavage product of VP4), rVP6 and the native VP7. PDI interaction with TLPs and rotavirus structural proteins was decreased by the presence of thiol/disulfide exchange inhibitors. Interactions of cell membrane-enriched fractions with TLPs produced rearrangements in the disulfide bridges of rotavirus structural proteins. We conclude that PDI interacts with rotavirus virions through redox reactions that could facilitate the rotavirus entry into the host cell.

Keywords: cell surface PDI; thiol-disulfide exchange; rotavirus TLPs; virus entry; bacitracin; DTNB

Introduction

Rotaviruses are the most frequent cause of severe and dehydrating diarrhea in infants and young children worldwide (Esposito *et al.*, 2011; Parashar *et al.*, 2006). Rotaviruses are formed by triple-layered particles (TLPs) where the outermost layer is composed by proteins VP7 and VP4 (including its trypsin cleavage products VP5* and VP8*) (Yeager *et al.*, 1990). The intermediate layer consists of VP6 while the inner layer is made of VP2 which encloses the 11-segmented dsRNA genome and minor proteins VP1 and VP3 (McClain *et al.*, 2010; Settembre *et al.*, 2011). Rotavirus entry into the host cell seems to include sequential interactions between virion proteins and several cell surface molecules (Isa *et al.*, 2008; Lopez and Arias, 2006). Internalization of virions into the target cell takes place through distinct endocytic pathways (Diaz-Salinas *et al.*, 2013, 2014). Conformational changes in VP4 have been involved in the host cell membrane distortion during entry (Dormitzer *et al.*, 2004; Rodriguez *et al.*, 2014). Evidence has been provided that VP4 (VP5* and VP8*), VP6 and VP7 are implicated in interactions with cell surface molecules as part of entry process (Gualtero *et al.*, 2007; Isa *et al.*, 2008). Rotavirus strains being N-acetyl neuraminic (sialic) acid (SA)-dependent/neuraminidase-

*Corresponding author: E-mail: caguerrerof@unal.edu.co; phone: +(57-1)-3165000 Ext. 15053.

Abbreviations: DLP = double-layered particles; HI = human rotavirus isolate; PDI = protein disulfide isomerase; SA = neuraminic (sialic) acid; TLP = triple-layered particles

sensitive bind first to SA through VP8*, whereas SA-independent/neuraminidase-insensitive strains interact directly with integrin α2β1 through VP5* (Isa *et al.*, 2006; Zarate *et al.*, 2000). However, there is evidence that SA is a key determinant for the initial interaction of both neuraminidase-sensitive and neuraminidase-insensitive rotavirus strains with the cell surface (Haselhorst *et al.*, 2009). It has been shown that human rotavirus strains specifically recognize A-type histo-blood group antigens (HBGAs) through VP8*, although major variations in their ability to recognize these antigens were detected (Bohm *et al.*, 2015). After binding to SA and integrin α2β1, rotavirus interacts with cell surface Hsc70 through VP5* and VP6 (Gualtero *et al.*, 2007; Guerrero *et al.*, 2002, 2012; Zarate *et al.*, 2003). Post-binding interactions implicating integrins α4β1, αxβ2 or αvβ3 are mediated by VP7 (Graham *et al.*, 2003; Hewish *et al.*, 2000; Zarate *et al.*, 2004). However, the sequence in which the post-binding interactions take place is still unknown. Recent evidence has indicated that rotaviruses also interact with cell surface protein disulfide isomerase (PDI) during the entry process since rotavirus infection is inhibited by membrane-impermeant thiol/disulfide exchange inhibitors, antibodies against PDI or cysteine-containing peptides derived from VP4 and VP7 (Calderón *et al.*, 2012a,b). Intracellular oxidant PDI has been found to be participating in the disulfide bond formation, folding and maturation of VP7 (Maruri-Avidal *et al.*, 2008; Mirazimi and Svensson, 1998; Svensson *et al.*, 1994). VP4, VP6, and VP7 contain cysteine residues susceptible to oxidation (i.e., disulfide-bond formation) (Aoki *et al.*, 2009; Patton *et al.*, 1993; Svensson *et al.*, 1994). However, crystallographic studies of VP6 (Mathieu *et al.*, 2001), VP8* (Dormitzer *et al.*, 2002) and VP5* (Dormitzer *et al.*, 2004; Yoder *et al.*, 2009) have shown that disulfide bonds are absent in these proteins. It has been suggested that rotavirus binding to cell surface receptors causes conformational changes in virion proteins and cell surface proteins Hsc70 and PDI are plausible candidates for inducing such changes (Calderón *et al.*, 2012 a,b; Perez-Vargas *et al.*, 2006).

PDI and thioredoxin-1 (Trx1) reduce the disulfide bonds present on HIV glycoprotein gp120 facilitating virus entry (Reiser *et al.*, 2012). Endothelial PDI has been involved in reducing integrins β1 and β3 causing the internalization of dengue virus (Wan *et al.*, 2012). The implication of PDI at the cell surface has been demonstrated in the entry of Sindbis virus where reduction of glycoprotein disulfide bonds is needed for virus membrane fusion (Abell and Brown, 1993). PDI family isomerases have been suggested to be responsible for the generation of free thiols in Newcastle disease virus (NDV) fusion (F) protein which is required for virus entry into cells and cell fusion (Jain *et al.*, 2007, 2008, 2009). Infection of HeLa cells by polyoma virus has been found to be facilitated by cell surface PDI (Gilbert *et al.*, 2006).

Understanding the molecular mechanisms underlying rotavirus-host cell interaction is crucial for the development of novel anti-rotaviral treatments for complementing vaccine approaches. The present study shows evidence that PDI interacts with rotavirus structural proteins VP7, VP6, and VP4 and that both soluble PDI and cell surface PDI-associated redox reaction is involved in modifying the redox status of these viral proteins.

Materials and Methods

Cells, animals, and viruses. MA104 cells were maintained in Advanced DMEM (Dullbecco´s modified Eagle´s medium (Sigma, USA) containing 2% FBS (Invitrogen, Carlsbad, USA). The cells were incubated in a CO_2 incubator at 37°C and 5% CO_2. Adult ICR mice (20–25 g; 4–5 weeks old) were purchased from the National Institute of Health, Bogotá, Colombia. Murine rotavirus strain ECwt (G3P [18]) (EDIM Cambridge wild type) was kindly donated by Dr. M. Franco (Genetics Institute, Pontificial Javerian University, Bogotá, Colombia) and propagated by orally inoculating suckling ICR mice (10–12 days old). Simian rotavirus strain RRV (P5B [3], G3) was kindly provided by Dr. C. F. Arias (Instituto de Biotecnología, Universidad Autónoma de México) and propagated in MA104 cells. One rotavirus isolate was isolated from fecal samples from a child affected with diarrhea in Bogotá. This isolate is hereafter referred to as human rotavirus isolate (HI). The present work was formally approved by the Ethical Committee of the School of Medicine, National University of Colombia, and performed according to the established guidelines.

Viral and cellular proteins. RRV VP7 was isolated from purified TLPs using SDS-PAGE in non-reductive conditions followed by electroelution (Electro-Eluter Bio-Rad, Hercules, USA). The electroeluted protein was characterized by Western blot analyses, precipitated with cold acetone, resuspended in PBS with 1 mM 2-mercaptoethanol (2-ME) and quantified using a NanoDrop® spectrophotometer (ND-1000, Thermo Scientific, USA). RRV recombinant proteins rVP5*, rVP6, and rVP8*, and rPDI and rHsc70 were obtained as previously reported (Moreno *et al.*, 2016). The purity of all proteins was assessed by SDS-PAGE in reducing conditions using silver staining.

Intestinal villus isolation. Mouse intestinal villus isolation was performed according to a previously reported method (Guerrero *et al.*, 2010). The final material containing intestinal villi was collected by low centrifugation, washed and resuspended in MEM containing antibiotic/antimycotic solution and kept at 4°C until use within 2 h. The viability of the villus-associated cells was determined using the trypan blue exclusion test. Ten representative photographs were taken and mean length of the villi measured.

Cell membrane isolation. Isolation of cell membrane-enriched fractions from intestinal villi was conducted as previously described (Lin *et al.*, 1987). Briefly, about 1.5 g of the isolated intestinal villi in hypotonic buffer (5 mM Hepes, 50 mM sucrose, pH 7.4) were homogenized during 15 min (Tissue Homogenizer, Tenbroeck, Ace Glass Inc., USA) with addition of $CaCl_2$ (10 mM final concentration) after 5 min from the start of homogenization. Membrane aggregates were spun down at 3,500 x *g* for 5 min at 4°C and the supernatant subjected to centrifugation at 20,000 x *g* for 30 min at 4°C. The pellet containing the cell membrane-enriched fraction was resuspended in sterile PBS (10 ml).

Virus purification. MA104 cells infected with RRV or small intestines from ECwt-infected mice were homogenized in MEM containing antibiotic/antimycotic solution and then subjected to two freeze-thaw cycles before extraction with 1,1,2-trichlorotrifluoroethane and sucrose/cesium chloride gradient centrifugation as previously described (Espejo *et al.*, 1981) with some modifications (Gualtero *et al.*, 2007). Nucleoprotein bands (TLPs and DLPs) were collected from the gradients by aspiration with a syringe, diluted with Tris-buffered saline (TBS) (10 mM Tris–HCl, pH 7.4, 150 mM NaCl, 1 mM $MgCl_2$, 5 mM $CaCl_2$) and submitted to centrifugation at 150,000 x *g* for 1.5 h at 4°C. The precipitated TLPs and DLPs were resuspended in sterile TBS and quantified spectrophotometrically (NanoDrop®). TLPs were converted into double-layered particles (DLPs) by treating TLPs with TBS containing 50 mM EDTA (TBS-E) without $CaCl_2$ and $MgCl_2$. TLPs in TBS-E were centrifuged at 100,000 x *g* for 1 h at 4°C through a 30% sucrose cushion. The precipitated DLPs were resuspended in TBS without $CaCl_2$ and $MgCl_2$, quantified using a NanoDrop® and stored at -70°C.

ELISA. Capture ELISA was conducted by coating 96-well microtiter plates with rabbit polyclonal antibodies against rotavirus structural proteins or against PDI overnight at 4°C. After washing three times with PBS-Tween (PBST) and blocking with 1% casein, the plates were incubated overnight at 4°C with either ultrasonic lysates in RIPA (20 mM Tris, pH 7.0, 130 mM NaCl, 10% glycerol, 1% NP-40, 1% Triton X-100, 0.1% sodium deoxycholate and 0.2 mg/ml PMSF) buffer from rotavirus-infected intestinal villi or cell membrane-enriched fractions that had been incubated with rotavirus particles. Plates were washed three times with PBST and then incubated with goat polyclonal antibodies against rotavirus or mouse mAb against PDI (Santa Cruz Biotechnology Inc., Santa Cruz, USA) for 1 h at 37°C. Plates were washed three times with PBST and then incubated with HRP-conjugated donkey anti-goat or anti-mouse secondary antibodies (Santa Cruz Biotechnology Inc.) for 1 h at 37°C. After washing three times with PBST, plates were incubated with 1 mg/ml o-phenylenediamine dihydrochloride (OPD) substrate in 50 mM sodium citrate buffer, pH 5.0, containing 0.05% H_2O_2. The reaction was stopped by the addition of 2.5 M H_2SO_4 and the plates were read at 492 nm in a microplate reader (Microplate Autoreader EL311-Bio-Tek Instruments, USA). Interaction of rPDI with TLPs, DLPs, and viral proteins was also measured by ELISA using microtiter plates coated with rPDI (40 μg/ml). Plates were washed three times with PBST and blocked with 0.5% casein in PBST for 2 h at 37°C. After washing three times with PBST, plates were either without incubation or incubated with the indicated concentrations of 5,5'-dithiobis(2-nitrobenzoic acid) (DTNB) or F(ab')2 from rabbit polyclonal anti-PDI antibodies (10 μg/ml) in PBST for 1 h at 37°C. Plates were washed three times with PBST and incubated with trypsin-activated TLPs [HI (130 μg/ml), ECwt (125 μg/ml) or RRV (150 μg/ml)], DLPs from ECwt and RRV at 150 μg/ml each, rVP5* (10 μg/ml), rVP6 (25 μg/ml), rVP8* (20 μg/ml) or VP7 (25 μg/ml) from RRV for 2 h at 37°C. Plates were washed three times with PBST and incubated with rabbit polyclonal antibodies to TLPs, rVP5*, rVP6* (which also detect DLPs), rVP8*, or VP7 for 1 h at 37°C. After washing three times with PBST, HRP-conjugated goat anti-rabbit secondary antibody (Santa Cruz Biotechnology Inc.) was added for 1 h at 37°C. The reaction was visualized with OPD. The mean absorbance values were obtained from three independent experiments conducted in duplicates.

Western blot analysis. RIPA-lysed villi or cell membrane-enriched fractions were incubated with protein A-Sepharose beads coupled with rabbit polyclonal antibodies against rotavirus structural proteins in PBS for 1 h at 37°C with constant agitation. Beads were washed three times with PBS and centrifuged at 2,500 x *g* for 3 min before adding Laemmli sample buffer and boiled for 5 min. Beads were collected by centrifugation at 2,500 x *g* for 3 min and the supernatant proteins were subjected to 10% SDS-PAGE and then transferred to a PVDF membrane using a semi-dry transfer apparatus (Bio-Rad) with transfer buffer (10 mM CAPS, pH 11, and 10% methanol). The membrane was blocked with 5% skimmed milk in PBST for 2 h at 37°C before incubation with goat anti-PDI serum (0.2 μg/ml) for 1 h at room temperature (RT). After washing three times with PBST, the membrane was incubated with HRP-conjugated rabbit anti-goat IgG (0.4 μg/ml, Santa Cruz Biotechnology Inc.) for 1 h at RT. The reaction was visualized using Western blot chemiluminescence luminol reagent (Santa Cruz Biotechnology Inc.) according to manufacturer's instructions. For detection of rotavirus structural proteins, the membrane was stripped in stripping buffer (62.5 mM Tris-HCl, pH 6.8, 100 mM 2-ME and 2% SDS in deionized water) for 45 min at 50°C. The membrane was washed five times with PBST for 10 min and blocked with 5% skimmed milk in PBST for 2 h at 37°C before being reprobed with goat primary antibodies against rotavirus virions. After washing with PBST, the membrane was incubated with HRP-conjugated donkey anti-goat secondary antibody for 1 h at 37°C and protein detection was performed using Chemiluminescence luminol reagent as indicated above.

Interaction of TLPs with cell membrane-associated PDI. Isolated intestinal villi (75 mg/ml total protein) in DMEM (100 ml/well) were incubated for 1 h at 4°C with 1/20 volume of trypsin-

activated HI, ECwt or RRV TLPs in final concentrations of 130, 125 and 150 µg/ml, respectively. Rotavirus TLP concentrations had the same MOI (multiplicity of infection) as determined in MA104 cells (data not shown). Preparations were further incubated for 5 or 15 min at 37°C and then collected by centrifugation at 2,500 × *g* for 3 min at 4°C. The villus pellet was washed three times with PBS to remove the unbound TLPs and then incubated in RIPA buffer for 40 min at 37°C under gentle agitation (100 rpm; UltraRocker rocking platform, Bio-Rad). Half of the lysate from villus cells was sonicated (Branson 250 Sonifier; output 20%, 3 30-sec pulses) and then subjected to immunodetection of PDI or TLPs by capture ELISA as described above. The remaining half of the lysate was subjected to immunoprecipitation using rabbit polyclonal antibodies against rotavirus structural proteins. The immunoprecipitated proteins were separated by SDS-PAGE and PDI was detected in Western blot analyses. The interaction of TLPs with PDI associated to cell membrane-enriched fraction was performed by mixing this fraction (20 mg/ml total protein) with TLPs at the final concentrations indicated above. Binding reactions were performed for 1 h at 4°C, whereas post-binding reactions took place for 5 min at 37°C. Unbound TLPs were washed out with sterile PBS by three cycles of centrifugation at 20,000 *g* for 15 min at 4°C, and the PBS-washed cell membrane-enriched fraction was lysed with RIPA buffer for 40 min at 37°C with gentle agitation. The presence of PDI or rotavirus structural proteins in the immunoprecipitated fractions were analyzed by capture ELISA and SDS-PAGE/Western blot analyses as indicated above.

Inhibition and reversion of PDI-rotavirus interaction. Intestinal villi (75 mg/ml total protein) or cell membrane-enriched fraction (2 mg/ml total protein) in DMEM (100 ml/well) were treated with bacitracin (7.5 mM) (Karala and Ruddock, 2010; Calderon *et al.,* 2012), DTNB (5 mM) (Winther and Thorpe, 2014; Calderon *et al*., 2012 a), NEM (20 mM) (Winther and Thorpe, 2014; Ruyechan, 1988) or rabbit F(ab')2 anti-PDI (10 or 20 µg/ml) in the indicated final concentrations which were obtained by adding a 1/20 volume of the corresponding stock solutions. The preparations in the presence of PMSF (0.2 mM) were kept at constant agitation (120 rpm) for 1 h at 37°C. Samples were subjected to three cycles of washing/centrifugation with PBS at 2,500 x *g* for 1 min or 20,000 x *g* for 15 min to remove agents from the villi and cell membrane-enriched fraction, respectively. The precipitated preparations were incubated with trypsin-activated HI (130 µg/ml), ECwt (125 µg/ml) or RRV (150 µg/ml) for 1 h at 4°C with gentle agitation before incubation for 5 min at 37°C. Unbound TLPs were removed from the villi and cell membrane-enriched fraction by three cycles of washing/centrifugation as indicated above. The precipitated preparations were lysed in RIPA buffer for 40 min at 37°C with gentle agitation. RIPA-lysed villus preparation was subjected to sonication as indicated above. Alternatively, intestinal villi were treated with the different TLPs for 1 h at 4°C followed by removing of unbound TLPs through three cycles of washing/centrifugation with PBS as indicated above. The villus pellet was resuspended in MEM and incubated for 5 min at 37°C before adding the thiol-disulfide interacting agents indicated above. After removing the agents by centrifugation through three cycles of washing/centrifugation with PBS, villi were lysed with RIPA buffer and sonicated. In all cases, PDI-TLP interaction was detected using capture ELISA as indicated above.

Redox changes in viral proteins. Labeling of TLPs with MPB [N^{α}-(3-maleimidylpropionyl)biocytin (Invitrogen™)] was essentialy performed as previously described (Jain *et al*., 2007; 2009). Briefly, MA104 cells in DMEM containing 0.2 mg/ml PMSF were left untreated or were treated with bacitracin (7.5 mM) or DTNB (7.5 mM) for 1 h at 37°C before centrifugation at 2,500 x *g* for 3 min at 4°C and resuspended in DMEM. The resuspended preparation at the protein concentration and volume indicated above was incubated with trypsin-activated HI (130 µg/ml) or RRV (150 µg/ml) in the presence of MPB (0.5 mM) (Jain *et al*., 2007) for 1 h at 4°C under constant agitation (120 rpm). MPB reaction was stopped by adding an equal volume of 0.5 mM NAC in PBS. Unbound TLPs and MPB were removed by washing with PBS and centrifugation as indicated above and the pellet was lysed with RIPA buffer for 40 min at 37°C with gentle agitation. The cell lysates were immunoprecipitated with protein A-Sepharose beads coupled with rabbit polyclonal antibodies against rotavirus structural proteins and processed as indicated for SDS-PAGE/Western blot analysis. Biotinylated proteins were probed with HRP-conjugated streptavidin (Invitrogen) and visualized with 3-amino-9-ethylcarbazole (AEC). Subsequent stripping of the membrane and reprobing with goat primary antibodies against rotavirus virions was performed as indicated above.

Detection of free thiols in viral proteins. For detection of free thiols in viral proteins, HI TLPs (130 µg/ml) in TBS were treated or left untreated with 5 mM dithiothreitol (DTT) for 1 h at 37°C. Excess of DTT was removed by submitting TLPs to centrifugation as indicated for TLP purification. TLPs were untreated or treated with 0.5 mM MPB for 30 min at RT with constant agitation. Unbound MPB was also removed by centrifugation as indicated for TLP purification and TLPs resuspended in TBS and immunoprecipitated with rabbit anti-rotavirus antibodies. The immunoprecipitated TLPs were denaturated with Laemmli sample buffer with 2-ME in a boiling water bath before analysis by SDS-PAGE/Western blot. Biotinylated proteins were detected with HRP-streptavidin conjugate and AEC as indicated above.

Statistical analysis. An unpaired Student's t-test was used to test for significant differences between treatments. Values were reported as mean ± SD and results were considered as not significant (ns) with $p > 0.05$, significant with $p < 0.05$, very significant with $p < 0.01$, and highly significant with $p < 0.001$. Statistical analysis was performed with GraphPad Prism® (Graphpad Software Inc., USA).

Results

Rotavirus binds cell membrane-associated PDI

To gain insight on the mechanisms mediating the interaction of rotavirus particles with the cell surface of enterocytes we used villi from small intestine which were isolated from ICR mice as previously reported (Guerrero *et al.*, 2010). The isolated small intestinal villi showed their typical morphology and mean size of about 196.7 ± 49.8 mM (Fig. 1a), with cell viability higher than 90% (data not shown). To test whether rotavirus virions bind to the cell surface PDI, TLPs from RRV, ECwt or HI were incubated with intestinal villi, followed by lysis with RIPA buffer, sonication and ELISA analysis for TLP-PDI interaction. Binding of TLPs to rHsc70 was used as a positive control (Arias *et al.*, 2002; Gualtero *et al.*, 2007; Guerrero *et al.*, 2012). Mean absorbance values from control wells containing sonicated RIPA lysates from untreated villi were subtracted from those of experimental absorbance values. When using capture antibodies against rotavirus, the resultant mean absorbance values for the detected PDI showed that in all the 3 rotaviruses tested PDI interacts with TLPs after 5 min incubation at 37°C (Fig. 1b). The mean ELISA absorbance values for PDI bound to RRV, ECwt, and HI were 0.568, 1.183 and 1.285 after 5 min incubation, respectively (Fig. 1b). However, after 15 min incubation at 37°C this binding tendency was only maintained for RRV (0.556) and HI (1.328) while significant decrease of bound PDI was observed for ECwt (0.651) (Fig. 1b). This might suggest that the ECwt interaction with cell surface PDI is more transient than that observed for RRV and HI. When using capture antibodies against PDI, the absorbance values for the RRV, ECwt and HI virions interacting with PDI were 0.350, 0.647 and 1.050 at 5 min incubation at 37°C, respectively. Again, a longer time of incubation (15 min) maintained the TLPs interaction with PDI only for RRV (0.428) and HI (1.150) whereas a significant decrease of the absorbance value for ECwt virions (0.189) bound with PDI was observed (Fig. 1b). This result suggests that ECwt virions could have been transited to other cell surface receptors after a longer incubation time.

To test whether rotaviruses interacted with PDI present in cell membrane-enriched fractions, TLPs from RRV, ECwt, and HI were incubated during 5 min at 37°C with cell-membrane-enriched fractions and their RIPA lysates were examined by ELISA. Mean absorbance values showed a significant interaction between PDI and TLPs from RRV (0.367), ECwt (0.398) and HI (0.717) (Fig. 1c). When RIPA lysates were captured by anti-PDI antibodies, the mean absorbance values for RRV (0.197), ECwt (0.306) and HI (0.448) interaction of TLPs with PDI were also significant (Fig. 1c). Rotavirus-rHsc70 interaction used as positive control showed mean absorbance values of 0.737 and 0.762 when capturing with anti-rotavirus or anti-Hsc70 antibodies, respectively (Fig. 1c). The ELISA results suggest that viral TLPs interact with PDI, although further experimental testing is needed for elucidating the details of this interaction.

PDI co-immunoprecipitates with TLPs

To further test for the PDI-TLP interaction, aliquots of the RIPA lysates from villi and membrane-enriched fractions were subjected to immunoprecipitation using polyclonal anti-rotavirus antibodies followed by Western blot analyses. The immunoprecipitated samples from villi that had been incubated 15 min at 37ºC with TLPs from RRV, ECwt or HI showed a positive reaction band at about 55 kDa after probing with anti-PDI antibodies (Fig. 1d, lanes 2, 4, 6), whereas no reaction was observed in lysates from samples without rotavirus (Fig. 1d, lane 1). Incubation of villi with the same TLPs during 5 min at 37ºC was also enough to show the same positive reaction for the PDI-TLP interaction (Fig. 1d, lanes 3, 5, 7). In the case of immunoprecipitated samples from RIPA lysates of cell-membrane-enriched fractions incubated with TLPs from ECwt or HI, a PDI positive reaction at about 55 kDa position was also observed (Fig. 1e, lanes 1, 3), while it was absent in samples without TLPs (Fig. 1e, lane 2). rPDI was used as a positive control (Fig. 1e, lane 5). Taken together, the immunoprecipitation results suggest that PDI can interact with TLPs either directly or indirectly through other rotavirus interacting proteins on the cell surface.

Antibodies to PDI inhibit rotavirus-PDI interaction

To test the specificity of PDI-TLP interaction, cell membrane-enriched fractions were treated with F(ab')2 of rabbit polyclonal anti-PDI antibodies, washed and then incubated with TLPs from RRV, ECwt or HI. After lysis with RIPA buffer, the samples were analyzed by ELISA using anti-rotavirus antibodies as capturing antibodies. The detection with goat anti-PDI antibodies showed that treatment of cell membrane-enriched fractions with F(ab')2 from anti-PDI antibodies (20 µg/ml) led to an inhibition of the PDI-TLP interaction of about 97, 89, and 79%, for RRV, ECwt, and HI, respectively, as compared with the mean absorbance values found in the samples from anti-PDI-untreated cell membrane-enriched fractions assumed as 100% PDI-TLP interaction (Fig. 1f). Pre-treatment of cell membrane-enriched fractions with a lower concentration of F(ab')2 of anti-PDI antibodies (10 µg/ml) was also enough to reduce the mean absorbance values of PDI bound to TLPs from RRV, ECwt, and HI by 88, 78,

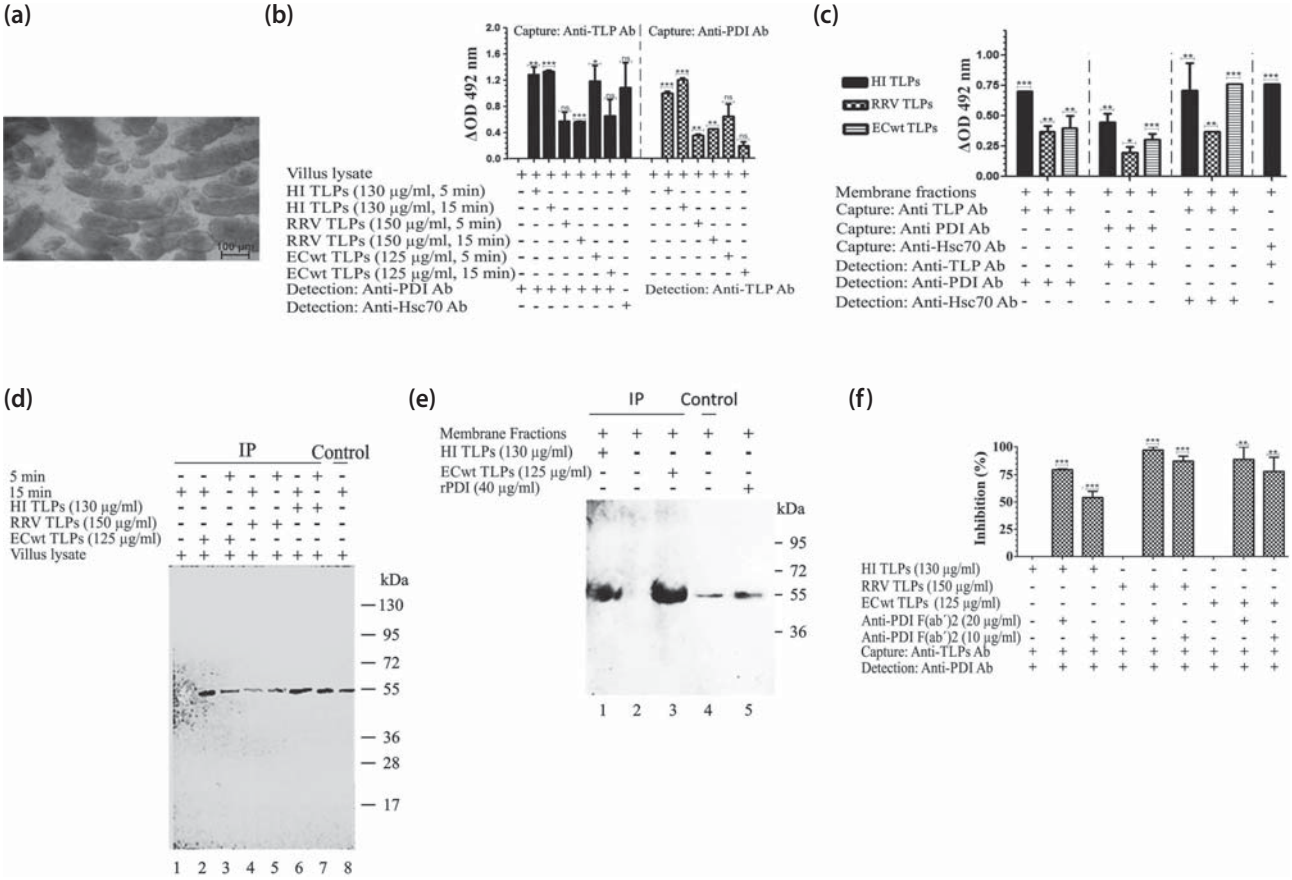

Fig. 1

PDI-TLP interaction on the cell surface and in cell membrane-enriched fractions

Intestinal villi from uninfected ICR mice or cell membrane-enriched fractions were incubated with rotavirus TLPs and analyzed with ELISA. **(a)** A representative image of small intestinal villi isolated from ICR mice. **(b)** PDI-TLP interaction in villus lysates. The interaction was determined using capture antibodies against rotavirus TLPs or against PDI. TLPs from RRV, ECwt or HI are indicated. The mean ΔOD values for PDI-TLP interaction are shown on the y-axis (ns = no significant difference; *p <0.05; **p <0.01; ***p <0.001). TLP-rHsc70 interaction was used as a positive control, and villus lysates without TLP treatment were used as a negative control. **(c)** PDI-TLP interaction from RIPA-solubilized cell membrane-enriched fractions. The interaction was determined using capture antibodies against rotavirus TLPs or against PDI. The TLPs from RRV, ECwt, and HI are indicated. Positive and negative controls, and mean ΔOD values were as described above. **(d)** Western blot analysis of co-immunoprecipitates (IP) from villus lysates. Villi were incubated with TLPs from the indicated rotaviruses and during the indicated times (min), lysed with RIPA buffer and immunoprecipitated with anti-rotavirus antibodies. The WB was performed using anti-PDI antibodies. RIPA lysates from TLP-untreated villi were used as a control. **(e)** Western blot analysis of co-immunoprecipitates obtained from RIPA-solubilized cell membrane-enriched fractions. A sample from a RIPA-solubilized cell membrane-enriched fraction without TLP treatment was used as a negative control. rPDI was used as a positive control. **(f)** Inhibition of PDI-TLP interaction by treatment with anti-PDI-F(ab')2. Cell membrane-enriched fraction was treated with anti-PDI-F(ab´)2 before incubation with the indicated TLPs. The RIPA-solubilized cell-membrane-enriched fractions were analyzed by ELISA using anti-rotavirus antibodies for capture and anti-PDI antibodies for detection. Cell membrane-enriched fractions without anti-PDI-F(ab´)2 treatment were used as a control. Data of inhibition of the PDI-TLP interaction derived from the mean ΔOD values are shown as mean inhibition percentage (±SD).

and 54%, respectively (Fig. 1f). These results suggest that PDI-TLP interaction could be specific, as it was practically abolished by F(ab')2 from anti-PDI antibodies.

PDI-TLP interaction involves thiol-disulfide exchange

To gain insight into the characterization of the nature of PDI-TLP interaction, isolated intestinal villi were treated with DTNB, bacitracin or NEM and then incubated with TLPs from RRV, ECwt or HI or DLPs from RRV or ECwt. Sonicated RIPA lysates were captured with anti-rotavirus or anti-PDI antibodies and correspondently detected with anti-PDI or anti-rotavirus antibodies. The mean absorbance values for PDI bound to TLPs were significantly reduced by pre-treatment with all the thiol-disulfide exchange reagents assayed leading to the corresponding significant inhibitions of the PDI-TLP interaction

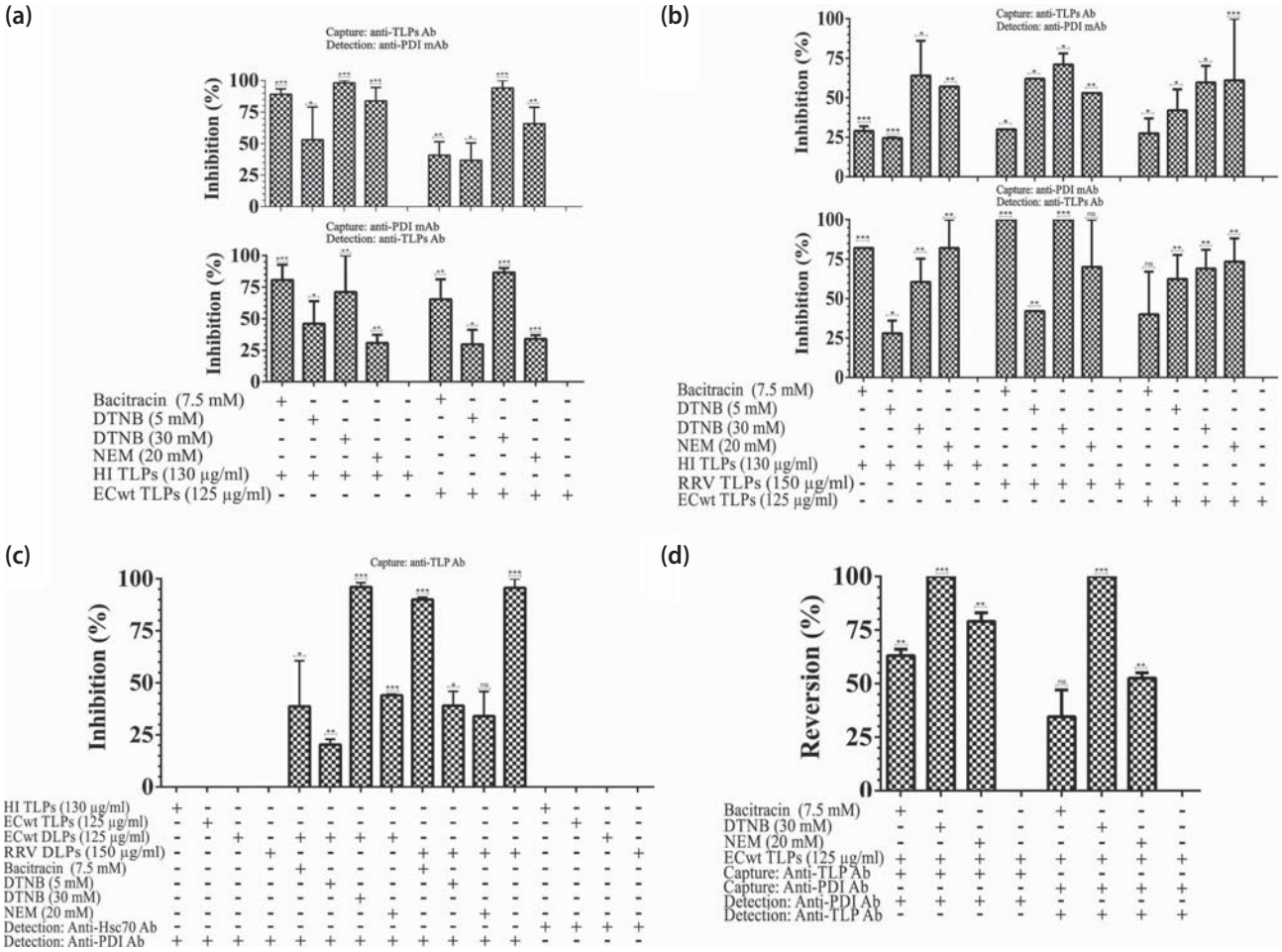

Fig. 2

Effect of thiol-disulfide exchange reagents on PDI-rotavirus interaction

(a) Inhibition of PDI-TLP interaction by treatment of villi with inhibitors of thiol-disulfide exchange. Small intestinal villi were incubated with bacitracin, DTNB, or NEM before incubation with TLPs from ECwt or HI. The PDI-TLP interaction was analyzed by ELISA in RIPA cell lysates captured with anti-TLP (top panel) or anti-PDI (bottom panel) antibodies and detected with the indicated antibodies. The reaction was developed with HRP-conjugated donkey anti-goat or anti-mouse secondary antibodies. The vertical axis indicates the percentage of the PDI-TLP interaction inhibition derived from the mean ΔOD values. Data are shown as mean (±SD) percentages (ns = no significant difference; *p <0.05; **p <0.01; ***p <0.001). **(b)** Inhibition of PDI-TLP interaction by treatment of cell membrane-enriched fractions with inhibitors of thiol-disulfide exchange. Cell membrane-enriched fractions were incubated with bacitracin, DTNB, or NEM before incubation with TLPs from RRV, ECwt or HI and the interaction was analyzed by ELISA using the indicated capture and detection antibodies. Data on the inhibition of PDI-TLP interaction are shown as indicated above. **(c)** Inhibition of PDI-DLP interaction by treatment with inhibitors of thiol-disulfide exchange. Cell membrane-enriched fractions were incubated with bacitracin, DTNB or NEM before incubation with DLPs from RRV or ECwt. The PDI-DLP interaction in the RIPA-solubilized cell membrane-enriched fractions was analyzed by ELISA using capture antibodies against TLPs which also recognize DLPs. The detection was performed with anti-PDI antibodies or anti-Hsc70 antibodies as a control. TLPs from ECwt and HI were also used as a control. Data on the inhibition percentages of the PDI-DLP interaction are shown as indicated above. **(d)** Reversion of the PDI-TLP interaction by treatment with thiol-disulfide exchange reagents. Small intestinal villi were incubated with TLPs from ECwt and analyzed by ELISA for the presence of PDI-TLP interaction after treatment with bacitracin, DTNB, or NEM. The capture and detection antibodies are indicated. The mean (±SD) percentages of the reversion of the PDI-TLP interaction derived from the mean ELISA ΔOD values are shown on the vertical axis.

in comparison with the untreated control villi (Fig. 2a). For instance, DTNB (5 mM) pre-treatment of villi caused inhibition of PDI-TLP interaction by about 30% for ECwt and 50% for HI independently of the antibodies used for capture or detection (Fig. 2a). Inhibition of interaction was further increased to more than 80% for both ECwt and HI when DTNB was increased to 30 mM (Fig. 2a). This suggests that free thiols in PDI seem to be needed for PDI-TLP interaction as the reaction between DTNB and thiol group results in the production of an equivalent amount

of 5-thio-2-nitrobenzoic acid. However, it has been reported that the DTNB method could underestimate the real concentration of thiol groups present in a protein due to its incomplete reaction (Faulstich *et al.*, 1993; Wright and Viola, 1998). Although the exact mechanism of DTNB binding to PDI is not completely elucidated, it has been demonstrated *in silico* that Cys37 of PDI plays an important role in its inhibition by DTNB binding during HIV infection (Gowthaman *et al.*, 2008). Bacitracin pre-treatment of villi decreased PDI-TLP interaction by about 89% and 80% for HI when anti-rotavirus or anti-PDI antibodies were used for capture in ELISA, respectively (Fig. 2a), this interaction was also decreased by 40% and 65% for ECwt, respectively (Fig. 2a). These results suggest that the reductive activity of PDI in the substrate-binding domain is involved in PDI-TLP interaction as bacitracin inhibits this activity (Dickerhof *et al.*, 2011). NEM pre-treatment of villi led to a significant reduction of the PDI-TLP interaction. Since NEM is used for detecting functional thiols in proteins, the results suggest that free thiols are required in PDI for interacting with TLPs.

PDI-TLP binding assays using RIPA lysates from cell membrane-enriched fractions instead of isolated intestinal villi showed that the mean ELISA absorbance values corresponding to PDI detected after capture with anti-rotavirus antibodies were significantly reduced by treatment with the thiol-disulfide exchange reagents tested. According to these absorbance values, bacitracin reduced PDI-TLP interaction for RRV, ECwt, and HI TLPs by 53, 70 and 34%, respectively; DTNB (5 mM) by 26, 58 and 52%, respectively; DTNB (30 mM) by 62, 85 and 65%, respectively; and NEM by 73, 58 and 67%, respectively, relative to cell membrane-enriched fractions that had not been treated with the thiol-disulfide exchange reagents (Fig. 2b). Regardless of whether anti-rotavirus or anti-PDI antibodies were used for capture, most of the thiol-disulfide exchange inhibitors used were able to cause inhibition of PDI-TLP interaction by at least 50% (Fig. 2b). The results obtained from cell membrane-enriched fractions also suggest that thiol-disulfide exchange is involved in PDI-TLP interaction. However, the remaining PDI-TLP interaction, whether direct or indirect, after pre-treatment with thiol-disulfide inhibitors could be explained by chaperone activity.

To test whether the PDI-DLP interaction is mediated by thiol-disulfide exchange, cell membrane-enriched fractions were pre-treated with DTNB, bacitracin, or NEM before the addition of RRV or ECwt DLPs. To test for PDI-DLP interaction, we took advantage of the fact that the serum raised against TLPs is reactive with all rotavirus structural proteins, including VP6. The mean absorbance values corresponding to PDI bound to DLPs captured by anti-rotavirus antibodies were significantly decreased and they corresponded to mean inhibitions of 30% (DTNB, 5 mM), 95% (DTNB, 30 mM), 70% (bacitracin), and 40% (NEM) for RRV and ECwt DLPs (Fig. 2c). Percentages were estimated relative to the mean absorbance values of PDI bound to DLPs from RRV or ECwt in control RIPA lysates from cell membrane-enriched fractions that had not been pre-treated with thiol-disulfide exchange inhibitors (Fig. 2c). These results indicate that VP6, the protein covering DLP surface, is interacting with PDI by a mechanism involving at least the thiol redox or disulfide exchange activities of PDI.

To test whether the TLP interaction with cell surface PDI could be reversed by addition of thiol-disulfide exchange inhibitor, isolated intestinal villi were first treated with ECwt TLPs. After removing the unbound TLPs, villi were treated with DTNB, bacitracin, or NEM at 4°C for 60 min. Sonicated RIPA lysates from villi were analyzed by ELISA using anti-rotavirus or anti-PDI antibodies for capture. Irrespectively of the capture or detection antibodies used, PDI-TLP interaction was reversed by 100% (DTNB), 50% (bacitracin), and 65% (NEM) (Fig. 2d). These results suggest that thiol groups in either viral proteins or PDI are needed for maintaining PDI-TLP interaction as DTNB and NEM react with thiol groups. Bacitracin effect on PDI-TLP interaction suggests that free cysteines are involved in maintaining this interaction. Assuming that the PDI-TLP interaction involves thiol-disulfide exchange reactions leading to the generation of free thiol groups in viral structural proteins and disulfide bonds in PDI active sites, a plausible interpretation of the effects caused by DTNB, NEM, and bacitracin treatments on this interaction could be made. After the PDI-TLP interaction is formed, it could be weakened by reacting free thiols in viral structural proteins through DTNB or NEM treatment. Since DTNB and NEM interfere with the enzymatic activities of PDI rather than with its chaperone activity, the residual PDI-TLP interaction could be attributed to PDI chaperone activity.

rPDI interacts with TLPs, DLPs, rVP5, rVP6, and rVP7

To test for a direct interaction between PDI and rotavirus virions or viral structural proteins, rPDI-coated ELISA plates were incubated with TLPs or DLPs from RRV, ECwt, HI or with rVP5*, rVP8*, rVP6 or VP7. The electrophoretic patterns of the rotavirus structural proteins tested are shown in Fig. 3a. The mean absorbance values of ELISA showed that TLPs from RRV (0.37), ECwt (0.43) and HI (0.9) were bound by rPDI as these absorbance values were obtained after subtracting those from control wells consisting of rPDI-coated and casein-blocked plates incubated with primary and secondary antibodies (Fig. 3b,

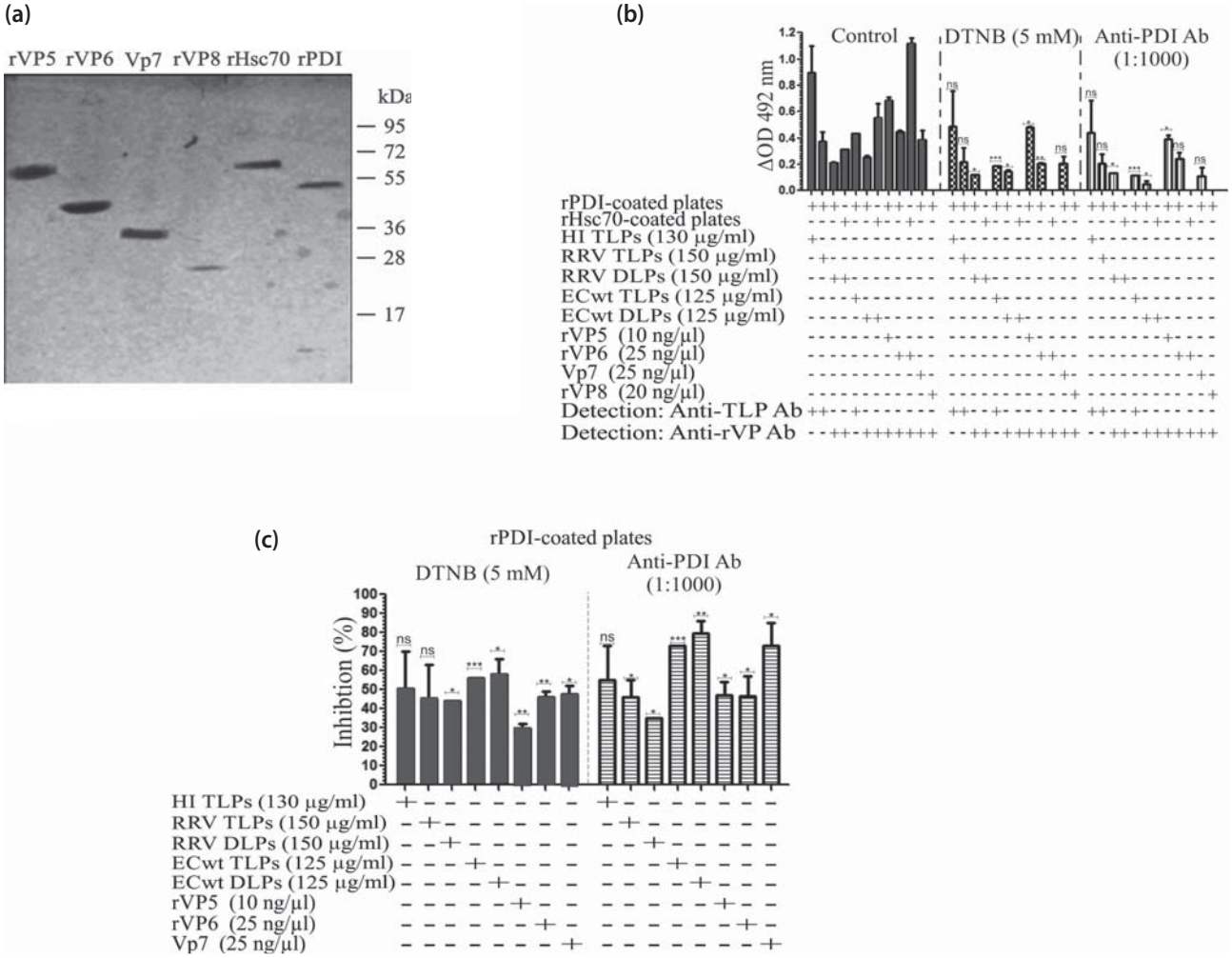

Fig. 3

***In vitro* interaction of rPDI with TLPs, DLPs, and rotavirus structural proteins**

(a) Electrophoretic profile of the rotavirus structural proteins. Purified rPDI, rVP5*, rVP8*, rVP6 and VP7 were analyzed by SDS-PAGE in reducing conditions and silver stained. **(b)** Interaction of rPDI with TLPs, DLPs, and rotavirus structural proteins. ELISA plates coated with rPDI were treated or left untreated (control) with DTNB or anti-PDI antibodies (F(ab')2) before incubation with TLPs, DLPs, rVP5*, rVP8*, rVP6, or VP7. The captured viral particles and proteins were detected with antibodies to TLPs (Anti-TLP Ab) and separate antibodies to rVP5*, rVP8*, rVP6 (which also detect DLPs), or VP7 labeled collectively as Anti-rVP Ab. Results are from three independent experiments performed in duplicates. The resultant mean ELISA ΔOD (±SD) values for interactions after subtracting the mean OD values from the control wells are shown (ns = no significant difference; *p <0.05; **p <0.01; ***p <0.001). **(c)** Inhibition percentages of the interaction of rPDI with TLPs, DLPs, rVP5*, rVP8*, rVP6 or VP7. The inhibition percentages of the interaction of rPDI with TLPs, DLPs, rVP5*, rVP6*, or VP7 caused by DTNB or F(ab')2 treatment were derived from the mean ELISA ΔOD values **(b)**. Data on inhibition are shown as mean (±SD) percentages.

left panel). Mean absorbance values for DLPs bound to rPDI were 0.21 (RRV) and 0.43 (ECwt) after subtracting mean absorbance values from the control wells (Fig. 3b, left panel). Positive control rHsc70-coated wells incubated with DLPs from RRV or ECwt showed mean absorbance values of 0.31 and 0.56, respectively (Fig. 3b, left panel). These results indicate that both TLPs and DLPs are significantly bound by rPDI. Mean absorbance values for RRV rVP5* (0.68), rVP8* (0.0), rVP6 (0.45) and VP7 (0.38) bound by rPDI (Fig. 3b) suggest that VP5* and VP7 could be responsible for the PDI-TLP interaction whereas PDI-DLP interaction could be mediated by VP6, the only accessible protein in DLPs). It is interesting to mention that rVP8* was unable to bind rPDI (Fig. 3b, left panel).

To gain insight into the basic mechanism mediating the direct interaction between rPDI and TLPs, DLPs or isolated viral structural proteins, rPDI-coated plates were pre-treated with DTNB or F(ab')2 from rabbit polyclonal anti-PDI antibodies before incubation with TLPs or DLPs from RRV, ECwt, HI, or with RRV rVP5*, rVP8*,

rVP6* or VP7. Mean absorbance values (Fig. 3b, central panel) indicated that DTNB pre-treatment reduced rPDI-TLP interaction by 45, 58 and 50% for RRV, ECwt and HI TLPs, respectively (Fig. 3c, left panel). According to the suggested inhibitory mechanism for DTNB, the results suggest that free thiols in PDI are needed to maintain PDI-TLP direct interaction, without excluding any PDI chaperone contribution.

Blocking rPDI-coated plates with anti-PDI F(ab')2 led to inhibition of PDI-TLP interaction by about 46, 73 and 55% for RRV, ECwt and HI, respectively (Fig. 3c, right panel), according to the absorbance values shown in Fig. 3b, right panel. Despite the lower molecular weight of F(ab')2 in comparison to the whole antibody, the results showed that its specific binding to PDI was able to interfere to a significant extent with the PDI-TLP interaction. However, the residual PDI-TLP interaction suggests that the level of steric hindrance caused by F(ab')2 was not enough to completely prevent this interaction. On the other hand, pre-treatment of rPDI with DTNB caused significant inhibition of the PDI interaction with rVP5*, rVP6, VP7 or DLPs. In all the cases, interactions were reduced by 50% in average in comparison to those observed for DTNB-untreated control rPDI (100%) (Fig. 3c, left panel). These results confirm the findings described above about the effect of DTNB treatment of villi on TLP binding that free thiol groups in PDI are required for binding of rotavirus structural proteins. Anti-PDI antibody pre-treatment of rPDI also led to more than 50% reduction of rPDI interactions with DLPs or the recombinant viral structural proteins tested, except for DLPs from RRV whose interaction with rPDI was only reduced by about 40% (Fig. 3c, right panel). The inhibitory effect on rPDI-DLP and rPDI-recombinant viral protein interactions caused by the F(ab') treatment of rPDI also indicate that this specific treatment was unable to completely interfere with these interactions probably due to insufficient steric hindrance.

Cell surface contact generates thiol groups in viral proteins

As mentioned above, VP4 (VP5* and VP8*), VP6 and VP7 have been reported to have cysteine residues susceptible to form disulfide bonds by oxidation (Aoki *et al.*, 2009; Patton *et al.*, 1993; Svensson *et al.*, 1994) although crystallographic studies have shown that disulfide bonds are absent in VP5*, VP8* and VP6 (Dormitzer *et al.*, 2004; Dormitzer *et al.*, 2002; Mathieu *et al.*, 2001; Yoder *et al.*, 2009). We wanted to determine whether thiol groups are exposed in HI TLP proteins using trypsin-activated TLPs with or without the treatment by reducing agent DTT. After incubating the DTT-treated TLPs with MPB, the analysis of TLP proteins by SDS-PAGE/Western blot under reducing conditions showed protein bands positive to the HRP-streptavidin conjugate with molecular sizes matching those of viral proteins (VP6 and VP7), independently whether or not the TLPs had been treated with trypsin (Fig. 4a, lanes 1, 2, 3, 8, 9). DTT-untreated TLPs that reacted with MPB did not show any protein band in the blot probed with HRP-streptavidin conjugate

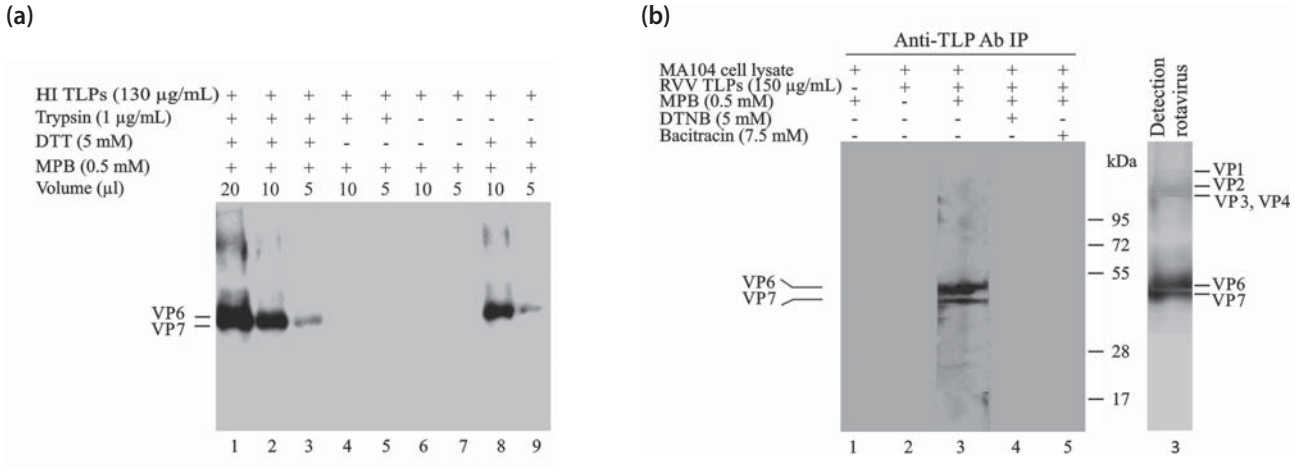

Fig. 4

Cell membrane-induced generation of thiol groups in rotavirus structural proteins

(a) Generation of thiols in rotavirus structural proteins by treatment with DTT. TLPs from HI were treated or left untreated with 5 mM DTT before treatment with MPB. The immunoprecipitated TLPs were analyzed by SDS-PAGE. **(b)** Generation of thiols in rotavirus structural proteins by contact with the cell surface. MA104 cells were treated with DTNB or bacitracin. After incubation with RRV TLPs and MPB, the cells were lysed in and immunoprecipitated with rabbit anti-rotavirus antibodies (Anti-TLP Ab). The rotavirus structural protein bands are shown on the right of the panel **(b)**.

(Fig. 4a, lanes 4, 5, 6, 7). These results suggest that native TLP proteins do not have free thiol groups available for reaction with MPB and that the MPB reactive sites were exposed following reduction with DTT. In addition, the results suggest that trypsin cleavage of VP4 does not lead to thiol group exposure in the cleavage products VP5* and VP8*.

To test whether the binding of RRV virions to MA104 cells leads to the generation of free thiols in viral structural proteins, cells were pre-treated with or without DTNB or bacitracin before incubation with RRV TLPs. After the reaction with MPB, the SDS-PAGE/Western blot analysis of the immunoprecipitated TLPs from RIPA lysates showed two protein bands interacting with HRP-streptavidin conjugate that were according to their sizes compatible with VP6 and VP7 (Fig. 4b, lane 3). These bands were absent in samples from MA104 cells that had been treated with DTNB or bacitracin before incubation with TLPs (Fig. 4b, lanes 1, 2). These bands were also absent in control samples in which MA104 cells were not incubated with TLPs or in MA104 cells incubated with TLPs but not treated with MPB (Fig. 4b, lanes 4, 5). These results suggest that thiol-disulfide exchange reactions are taking place in the cell surface membrane, leading to the generation of free thiol groups in viral proteins. PDI and other related thioredoxins are plausible candidates for performing these reactions (Calderon *et al.*, 2012a). After stripping off the HRP-streptavidin conjugate, the membrane was probed with primary anti-rotavirus antibodies. After visualization of the reaction products, it was found that all rotavirus structural proteins were revealed (Fig. 4b, lane 3, right panel) and that, according to their electrophoretic mobility, the protein bands reacting with MPB (Fig. 4b, lane 3, left panel) corresponded to VP6 and VP7 (Fig. 4b, lane 3, right panel). This result confirms that disulfide bonds present in these viral structural proteins were reduced by thiol-disulfide isomerases present in the cell surface of the target cell.

Discussion

Previous work has shown that rotaviruses seem to interact with multiple cell surface molecules either sequentially or alternatively in order to enter the host cell (Guerrero and Acosta, 2016; Lopez and Arias, 2006). Among these cell surface molecules, PDI has been reported to be used by rotaviruses (Calderon *et al.*, 201a). In this report, we started from the hypothesis that the reducing cell surface PDI, or even integrin αvβ3 or another thioredoxin, is able to induce thiol-disulfide exchange in rotavirus structural proteins for providing conformational changes needed for entry.

Our findings indicate that DTNB, a membrane-impermeant reagent that reacts with free thiols (Feener *et al.*, 1990), was able to inhibit the PDI-TLP interaction arising during the contact of rotavirus particles with either the cell surface or cell membrane-enriched fractions from MA104 cells. This inhibitory effect suggests that the cell surface membrane-associated reductive activity involved in the reduction of disulfide bridges has been significantly abolished by the DTNB pretreatment of cells. However, the residual PDI-TLP interaction detected after DTNB pretreatment might be attributed to an eventual PDI chaperone activity. In addition, the NEM pretreatment of the cells or cell membrane-enriched fractions led also to significant inhibition of the PDI-TLP interaction. This result also suggests the implication of thiol groups in this interaction as NEM reacts with functional thiols in proteins (Winther and Thorpe, 2014; Ruyechan, 1988).

The fact that the native TLP structural proteins lack reacting thiols in the absence of DTT pretreatment and that MPB reacting thiols are formed in the VP6 and VP7 structural proteins after the TLP contact with the cell surface suggests that the PDI-TLP interaction could lead to the formation of these thiol groups in the viral proteins. The occurrence of this redox reaction is further supported by the inhibition of the PDI-TLP interaction caused by the DTNB and NEM pretreatments of cells. On the other hand, bacitracin, a non-specific membrane-impermeant thiol/disulfide exchange inhibitor, was also able to inhibit the PDI-TLP interaction. The interfering effect of bacitracin on the PDI-TLP interaction could be explained in terms of the inhibition of the reductive activity of PDI needed to generate free thiol groups in the viral structural proteins with the consequent production of disulfide bridges in the active site of PDI.

From the angle of the potential PDI substrates in the rotavirus TLPs, VP4 (VP5* and VP8*), VP6 and VP7 have been reported to contain cysteine residues capable of forming disulfide bridges (Patton *et al.*, 1993; Svensson *et al.*, 1994; Aoki *et al.*, 2009). However, crystallographic studies have shown that the cysteine residues present in VP5* (Dormitzer *et al.*, 2004; Yoder *et al.*, 2009), VP8* (Dormitzer *et al.*, 2002) and VP6 (Mathieu *et al.*, 2001) are not forming disulfide bridges. The absence of disulfide bridges in the VP5* and VP8* structural proteins of TLPs suggest that these proteins could not be substrates of the reductive activity of the cell surface PDI. On the other hand, the lack of disulfide bridges in the VP6 structural protein forming the DLP surface would not make it a substrate for reductive activity of the cell surface PDI assumed to be implicated in the PDI-DLP complex formation. However, our results suggest that free thiols in the cell surface PDI, which are associated with its reductive activity, were needed for maintaining the PDI-DLP interaction

as this interaction was significantly inhibited by DTNB and NEM pre-treatment of the cells. Our interpretation of this result is that VP6 certainly contains at least one disulfide bridge as DTT treatment of the virus particles resulted in the generation of free thiols as suggested by the VP6 reactivity with MPB only after treatment with DTT. Then, it sounds plausible to propose that the redox activity of PDI is involved in maintaining the PDI-DLP interaction. Of course, it cannot be ruled out that in the PDI-DLP interaction the highly trimeric and hydrophobic VP6 covering the DLP surface is playing an additional role as a potential substrate of the PDI chaperone activity.

In the case of VP7, this TLP structural protein contains disulfide bridges (Svensson *et al*., 1994; Aoki *et al*., 2009) which are generated by the oxidant PDI present in the endoplasmic reticulum (ER) (Mirazimi and Svensson, 1998). This structural characteristic of VP7 allows us to suggest that the PDI-TLP interaction is mainly mediated by the reductive activity of the cell surface PDI, because this interaction was significantly disrupted by DTNB, NEM or bacitracin treatment of the cell before the addition of TLPs. The PDI-TLP complex might be maintained by disulfide bonds between PDI and cysteine-containing TLP proteins or by weak interactions mediating PDI chaperone activity. However, the inhibition of the PDI-TLP complex formation by DTNB, NEM, and bacitracin suggests that a thiol-disulfide exchange in which disulfide bonds are cleaved by the thiols present in the active site of the reductive PDI is occurring. VP7 is the most likely candidate for being a substrate of the reductive activity of the cell surface PDI as VP7 contains four disulfide bonds (Aoki *et al*., 2009).

The fact that DTNB and bacitracin treatments of cells were able to inhibit the free thiol generation in VP6 and VP7 upon the TLP contact with the cell surface suggests that thiol-disulfide exchange reactions are taking place during attachment of virus particles to the cell surface. Although PDI-TLP direct interaction occurs as shown in the present work, the non-specific inhibitory nature of DTNB and bacitracin leaves room for considering the participation of additional members of the thioredoxin family in the TLP-cell surface interaction that were not studied in the present work. It has been shown that the F protein on the surface of the Newcastle disease virus is reduced by cell surface thiol-disulfide isomerases to generate free thiols (Jain *et al*., 2009). On the other hand, rotavirus entry into the host cell has been shown to be dependent on the thiol-disulfide exchange activity on the cell surface (Calderon *et al*., 2012a). The reductive activity of the cell surface PDI and other thioredoxins has been also shown in the cleavage of disulfide bonds in membrane-bound ligands (Mandel *et al*., 1993) and in the HIV-1 envelope protein (Env) (Markovic *et al*., 2004; Ou *et al*., 2006; Auwerx *et al*., 2009). It has been proposed that TLP binding to the cell surface produces conformational changes in the viral structural proteins which are needed for entry (Arias *et al*., 2002). PDI and Hsc70 have been identified as candidates for causing these conformational changes (Calderon *et al*., 2012a; Pérez-Vargas *et al*., 2006; Guerrero and Acosta, 2016).

It is interesting to note that the PDI-TLP interaction appears not to be maintained by an irreversible covalent enzyme-substrate intermediate as the binding of TLPs to the cell surface is reversed by DTNB, NEM or bacitracin treatment. Although it has been reported that DTNB not only reacts with free thiols but also breaks disulfide bonds by a thiol-disulfide reaction (Schauenstein *et al*., 1982), it seems to be more plausible to suggest that PDI-TLP interaction on the cell surface is a reversible reaction that would allow for interconversion between the reduced and oxidized forms of the substrate and enzyme. In our experimental conditions, this reversibility of the reaction would allow interaction of the inhibitors with PDI after TLP binding. However, the understanding of the detailed molecular mechanisms involved in the reversion of the PDI-TLP interaction needs further research.

Overall, the participation of PDI during the rotavirus entry into the target cells gains support from the present results as the DTNB and bacitracin treatment of cells inhibited the formation of the PDI-TLP complex and also inhibited the rotavirus infectivity as previously shown (Calderon *et al*., 2012a). In addition, at least the disulfide bond-containing VP7 is a potential substrate of the reductive PDI or another cell surface thioredoxin able to generate free thiols after TLP contact with the cell surface. However, further research is needed to identify the complete set of cell surface molecules and the sequence of their use during rotavirus entry, including those responsible for thiol-disulfide exchange reactions.

References

Abell BA, Brown DT (1993): Sindbis virus membrane fusion is mediated by reduction of glycoprotein disulfide bridges at the cell surface. J. Virol. 67, 5496–5501. https://doi.org/10.1128/JVI.67.9.5496-5501.1993

Aoki ST, Settembre EC, Trask SD, Greenberg HB, Harrison SC, Dormitzer PR (2009): Structure of rotavirus outer-layer protein VP7 bound with a neutralizing Fab. Science 324, 1444–1447. https://doi.org/10.1126/science.1170481

Auwerx J, Isacsson O, Söderlund J, Balzarini J, Johansson M, Lundberg M (2009): Human glutaredoxin-1 catalyzes the reduction of HIV-1 gp120 and CD4 disulfides and its inhibition reduces HIV-1 replication. Int. J. Biochem. Cell. Biol. 41, 1269–1275. https://doi.org/10.1016/j.biocel.2008.10.031

Arias CF, Isa P, Guerrero CA, Mendez E, Zarate S, Lopez T, Espinosa R, Romero P, Lopez S (2002): Molecular biology of rotavirus cell entry. Arch. Med. Res. 33, 356–361. https://doi.org/10.1016/S0188-4409(02)00374-0

Bohm R, Fleming FE, Maggioni A, Dang VT, Holloway G, Coulson BS, von Itzstein M, Haselhorst T (2015): Revisiting the role of histo-blood group antigens in rotavirus host-cell invasion. Nat. Commun. 6, 5907. https://doi.org/10.1038/ncomms6907

Calderon MN, Guerrero CA, Acosta O, Lopez S, Arias CF (2012a): Inhibiting rotavirus infection by membrane-impermeant thiol/disulfide exchange blockers and antibodies against protein disulfide isomerase. Intervirology 55, 451–464. https://doi.org/10.1159/000335262

Calderón M, Guzmán F, Acosta O, Guerrero, C (2012b): Rotavirus VP4 and VP7-derived synthetic peptides as potential substrates of protein disulfide isomerase lead to inhibition of rotavirus infection. Int. J. Pept. Res. Ther. 18, 373–382. https://doi.org/10.1007/s10989-012-9314-z

Diaz-Salinas MA, Romero P, Espinosa R, Hoshino Y, Lopez S, Arias CF (2013): The spike protein VP4 defines the endocytic pathway used by rotavirus to enter MA104 cells. J. Virol. 87, 1658–1663. https://doi.org/10.1128/JVI.02086-12

Diaz-Salinas MA, Silva-Ayala D, Lopez S, Arias CF (2014): Rotaviruses reach late endosomes and require the cation-dependent mannose-6-phosphate receptor and the activity of cathepsin proteases to enter the cell. J. Virol. 88, 4389–4402. https://doi.org/10.1128/JVI.03457-13

Dickerhof N, Kleffmann T, Jack R, McCormick S (2011): Bacitracin inhibits the reductive activity of protein disulfide isomerase by disulfide bond formation with free cysteines in the substrate-binding domain. FEBS J. 278, 2034–2043. https://doi.org/10.1111/j.1742-4658.2011.08119.x

Dormitzer PR, Nason EB, Prasad BV, Harrison SC (2004): Structural rearrangements in the membrane penetration protein of a non-enveloped virus. Nature 430, 1053–1058. https://doi.org/10.1038/nature02836

Dormitzer PR, Sun ZY, Wagner G, Harrison SC (2002): The rhesus rotavirus VP4 sialic acid binding domain has a galectin fold with a novel carbohydrate binding site. EMBO J. 21, 885–897. https://doi.org/10.1093/emboj/21.5.885

Espejo R, Lopez S, Arias CF (1981): Structural polypeptides of simian rotavirus SA11 and the effect of trypsin. J. Virol. 37, 156–160 https://doi.org/10.1128/JVI.37.1.156-160.1981

Esposito DH., Holman RC, Haberling DL, Tate JE, Podewils LJ, Glass RI, Parashar U (2011): Baseline estimates of diarrhea-associated mortality among United States children before rotavirus vaccine introduction. Pediatr. Infect. Dis. J. 30, 942–947. https://doi.org/10.1097/INF.0b013e3182254d19

Faulstich H, Tews P, Heintz D (1993): Determination and derivatization of protein thiols by n-octyldithionitrobenzoic acid. Anal. Biochem. 208, 357–362. https://doi.org/10.1006/abio.1993.1061

Feener EP, Shen WC, Ryser HJ (1990): Cleavage of disulfide bonds in endocytosed macromolecules. A processing not associated with lysosomes or endosomes. J. Biol. Chem. 265, 18780–18785.

Gilbert J, Ou W, Silver J, Benjamin T (2006): Downregulation of protein disulfide isomerase inhibits infection by the mouse polyomavirus. J. Virol. 80, 10868–10870. https://doi.org/10.1128/JVI.01117-06

Gowthaman U, Jayakanthan M, Sundar D (2008): Molecular docking studies of dithionitrobenzoic acid and its related compounds to protein disulfide isomerase: computational screening of inhibitors to HIV-1 entry. BMC Bioinformatics 9 (Suppl. 12), S14. https://doi.org/10.1186/1471-2105-9-S12-S14

Graham KL, Halasz P, Tan Y, Hewish MJ, Takada Y, Mackow ER, Robinson MK, Coulson BS (2003): Integrin-using rotaviruses bind alpha2beta1 integrin alpha2 I domain via VP4 DGE sequence and recognize alphaXbeta2 and alphaVbeta3 by using VP7 during cell entry. J. Virol. 77, 9969–9978. https://doi.org/10.1128/JVI.77.18.9969-9978.2003

Gualtero DF, Guzman F, Acosta O, Guerrero CA (2007): Amino acid domains 280-297 of VP6 and 531-554 of VP4 are implicated in heat shock cognate protein hsc70-mediated rotavirus infection. Arch. Virol. 152, 2183–2196. https://doi.org/10.1007/s00705-007-1055-5

Guerrero CA, Acosta O (2016): Inflammatory and oxidative stress in rotavirus infection. World J. Virol. 5, 38–62. https://doi.org/10.5501/wjv.v5.i2.38

Guerrero CA, Bouyssounade D, Zarate S, Isa P, Lopez T, Espinosa R, Romero P, Mendez E, Lopez S, Arias CF (2002): Heat shock cognate protein 70 is involved in rotavirus cell entry. J. Virol. 76, 4096–4102. https://doi.org/10.1128/JVI.76.8.4096-4102.2002

Guerrero CA, Santana AY, Acosta O (2010): Mouse intestinal villi as a model system for studies of rotavirus infection. J. Virol. Methods 168, 22–30. https://doi.org/10.1016/j.jviromet.2010.04.010

Guerrero CA, Moreno LP (2012): Rotavirus receptor proteins Hsc70 and integrin αvβ3 are located in the lipid microdomains of animal intestinal cells. Acta Virol. 56, 63–70. https://doi.org/10.4149/av_2012_01_63

Haselhorst T, Fleming FE, Dyason JC, Hartnell RD, Yu X, Holloway G, Santegoets K, Kiefel MJ, Blanchard H, Coulson BS, von Itzstein M (2009): Sialic acid dependence in rotavirus host cell invasion. Nat. Chem. Biol. 5, 91–93. https://doi.org/10.1038/nchembio.134

Hewish MJ, Takada Y, Coulson BS (2000): Integrins alpha2beta1 and alpha4beta1 can mediate SA11 rotavirus attachment and entry into cells. J. Virol. 74, 228–236. https://doi.org/10.1128/JVI.74.1.228-236.2000

Isa P, Arias CF, Lopez S (2006): Role of sialic acids in rotavirus infection. Glycoconj. J. 23, 27–37. https://doi.org/10.1007/s10719-006-5435-y

Isa P, Gutierrez M, Arias CF, Lopez S (2008): Rotavirus cell entry. Future Virol. 3, 135–146. https://doi.org/10.2217/17460794.3.2.135

Jain S, McGinnes LW, Morrison TG (2007): Thiol/disulfide exchange is required for membrane fusion directed by

the Newcastle disease virus fusion protein. J. Virol. 81, 2328–2339. https://doi.org/10.1128/JVI.01940-06

Jain S, McGinnes LW, Morrison TG (2008): Overexpression of thiol/disulfide isomerases enhances membrane fusion directed by the Newcastle disease virus fusion protein. J. Virol. 82, 12039–12048. https://doi.org/10.1128/JVI.01406-08

Jain S, McGinnes LW, Morrison TG (2009): Role of thiol/disulfide exchange in Newcastle disease virus entry. J. Virol. 83, 241–249. https://doi.org/10.1128/JVI.01407-08

Karala AR, Ruddock LW (2010): Bacitracin is not a specific inhibitor of protein disulfide isomerase. FEBS J. 277, 2454–2462. https://doi.org/10.1111/j.1742-4658.2010.07660.x

Lin PH, Selinfreund R, Wakshull E, Wharton W (1987): Rapid and efficient purification of plasma membrane from cultured cells: characterization of epidermal growth factor binding. Biochemistry 26, 731–736. https://doi.org/10.1021/bi00377a012

Lopez S, Arias CF (2006): Early steps in rotavirus cell entry. Curr. Top Microbiol. Immunol. 309, 39–66. https://doi.org/10.1007/3-540-30773-7_2

Mandel R, Ryser JH, Ghani F, Wu M, Peak D (1993): Inhibition of a reductive function of the plasma membrane by bacitracin and antibodies against protein disulfide-isomerase. Proc. Natl. Acad. Sci. USA 90, 4112–4116. https://doi.org/10.1073/pnas.90.9.4112

Markovic I, Stantchev TS, Fields KH, Tiffany LJ, Tomic M, Weiss CD, Broder CC, Strebel K, Clouse KA (2004): Thiol/disulfide exchange is a prerequisite for CXCR4-tropic HIV-1 envelope-mediated T-cell fusion during viral entry. Blood 103, 1586–1594. https://doi.org/10.1182/blood-2003-05-1390

Maruri-Avidal L, Lopez S, Arias CF (2008): Endoplasmic reticulum chaperones are involved in the morphogenesis of rotavirus infectious particles. J. Virol. 82, 5368-5380. Mathieu M, Petitpas I, Navaza J, Lepault J, Kohli E, Pothier P, Prasad BV, Cohen J, Rey FA (2001): Atomic structure of the major capsid protein of rotavirus: implications for the architecture of the virion. EMBO J. 20, 1485–1497. https://doi.org/10.1128/JVI.02751-07

McClain B, Settembre E, Temple BR, Bellamy AR, Harrison SC (2010): X-ray crystal structure of the rotavirus inner capsid particle at 3.8 A resolution. J. Mol. Biol. 397, 587–599. https://doi.org/10.1016/j.jmb.2010.01.055

Mirazimi A, Wan L (1998): Carbohydrates facilitate correct disulfide bond formation and folding of rotavirus VP7. J. Virol. 72, 3887–3892. https://doi.org/10.1128/JVI.72.5.3887-3892.1998

Moreno LY, Guerrero CA, Acosta O (2016): Protein disulfide isomerase and heat shock cognate protein 70 interactions with rotavirus structural proteins using their purified recombinant versions. Rev. Colomb. Biotecnol. 18, 33–48. https://doi.org/10.15446/rev.colomb.biote.v18n1.57714

Ou W, Silver J (2006): Role of protein disulfide isomerase and other thiol-reactive proteins in HIV-1 envelope protein-mediated fusion. Virology 350, 406–417. https://doi.org/10.1016/j.virol.2006.01.041

Parashar UD, Gibson CJ, Bresee JS, Glass RI (2006): Rotavirus and severe childhood diarrhea. Emerg. Infect. Dis. 12, 304–306. https://doi.org/10.3201/eid1202.050006

Patton JT, Hua J, Mansell EA (1993): Location of intrachain disulfide bonds in the VP5* and VP8* trypsin cleavage fragments of the rhesus rotavirus spike protein VP4. J. Virol. 67, 4848–4855. https://doi.org/10.1128/JVI.67.8.4848-4855.1993

Perez-Vargas J, Romero P, Lopez S, Arias CF (2006): The peptide-binding and ATPase domains of recombinant hsc70 are required to interact with rotavirus and reduce its infectivity. J. Virol. 80, 3322–3331. https://doi.org/10.1128/JVI.80.7.3322-3331.2006

Reiser K, Francois KO, Schols D, Bergman T, Jornvall H, Balzarini J, Karlsson A, Lundberg M (2012): Thioredoxin-1 and protein disulfide isomerase catalyze the reduction of similar disulfides in HIV gp120. Int. J. Biochem. Cell Biol. 44, 556–562. https://doi.org/10.1016/j.biocel.2011.12.015

Rodriguez JM, Chichon FJ, Martin-Forero E, Gonzalez-Camacho F, Carrascosa JL, Caston JR, Luque D (2014): New insights into rotavirus entry machinery: stabilization of rotavirus spike conformation is independent of trypsin cleavage. PLoS Pathog. 10, e1004157. Ruyechan WT (1988): N-ethylmaleimide inhibition of the DNA-binding activity of the herpes simplex virus type 1 major DNA-binding protein. J. Virol. 62, 810–817 PMID: 28286. https://doi.org/10.1371/journal.ppat.1004157

Schauenstein E, Sorger S, Reiter M, Dachs F (1982): Free thiol groups and labile disulfide bonds in the IgG fraction of human serum. J. Immunol. Methods 50, 51–56. PMID: 7086149. https://doi.org/10.1016/0022-1759(82)90303-9

Settembre EC, Chen JZ, Dormitzer PR, Grigorieff N, Harrison SC (2011): Atomic model of an infectious rotavirus particle. EMBO J. 30, 408–416. https://doi.org/10.1038/emboj.2010.322

Svensson L, Dormitzer PR, von Bonsdorff CH, Maunula L, Greenberg HB (1994): Intracellular manipulation of disulfide bond formation in rotavirus proteins during assembly. J. Virol. 68, 5204–5215. https://doi.org/10.1128/JVI.68.8.5204-5215.1994

Wan SW, Lin CF, Lu YT, Lei HY, Anderson R, Lin YS (2012): Endothelial cell surface expression of protein disulfide isomerase activates ss 1 and ss 3 integrins and facilitates dengue virus infection. J. Cell. Biochem. 113, 1681–1691. https://doi.org/10.1002/jcb.24037

Winther JR, Thorpe C (2014): Quantification of thiols and disulfides. Biochim. Biophys. Acta 1840, :838–846 . https://doi.org/10.1016/j.bbagen.2013.03.031

Wright SK, Viola RE (1998): Evaluation of methods for the quantitation of cysteines in proteins. Anal. Biochem. 265, 8–14. https://doi.org/10.1006/abio.1998.2858

Yeager M, Dryden KA, Olson NH, Greenberg HB, Baker TS (1990): Three-dimensional structure of rhesus rotavirus by cryoelectron microscopy and image reconstruction. J. Cell Biol. 110, 2133–2144. https://doi.org/10.1083/jcb.110.6.2133

Yoder JD, Trask SD, Vo TP, Binka M, Feng N, Harrison SC, Greenberg HB, Dormitzer PR (2009): VP5* rearranges when rotavirus uncoats. J. Virol. 83, 11372–11377. https://doi.org/10.1128/JVI.01228-09

Zarate S, Cuadras MA, Espinosa R, Romero P, Juarez KO, Camacho-Nuez M, Arias CF, Lopez S (2003): Interaction of rotaviruses with Hsc70 during cell entry is mediated by VP5. J. Virol. 77, 7254–7260. https://doi.org/10.1128/JVI.77.13.7254-7260.2003

Zarate S, Espinosa R, Romero P, Mendez E, Arias CF, Lopez S (2000): The VP5 domain of VP4 can mediate attachment of rotaviruses to cells. J. Virol. 74, 593–599. https://doi.org/10.1128/JVI.74.2.593-599.2000

Zarate S, Romero P, Espinosa R, Arias CF, Lopez S (2004): VP7 mediates the interaction of rotaviruses with integrin alphavbeta3 through a novel integrin-binding site. J. Virol. 78, 10839–10847. https://doi.org/10.1128/JVI.78.20.10839-10847.2004